Vol. 19(1), pp. 1-11, January-March, 2024
DOI: 10.5897/IJPS2023.5047
Article Number: E20F24C71810
ISSN: 1992-1950

http://www.academicjournals.org/IJPS

ACADEMIC JOURNALS
expand your knowledge

International Journal of Physical Sciences

Full Length Research Paper

Mapping of geological structures controlling mineralization in parts of the Lower Benue Trough, Nigeria, using high resolution aeromagnetic data

Chukwuebuka J. Magbo* and Chukwudi C. Ezeh

Department of Geology and Mining, Enugu State University of Science and Technology, Enugu, Nigeria.

Received 8 September, 2023; Accepted 22 January, 2024

Nine Regional Aeromagnetic data sheets from the Lower Benue Trough, Nigeria have been interpreted using the centroid and forward modelling technique of spectral analysis with the aim of delineating structures that can possibly control mineralization within the trough. The residual magnetic map was analyzed using the geological cross-section to determine the number of anomalies and the Fourier transform method was used to estimate the depth to the top and bottom of the anomaly, the analytical signal amplitude, the first vertical derivative, Rose diagram and power spectrum. From the spectral analysis results, the estimated depth value to the top of the anomalous body ranges from 0.5 km to about 12 km, with the highest depth to the top of the anomaly located within the south-western and north-western axis of the study area. The estimated depth to the bottom of the anomalous body ranges from about 20 to 50 km with the highest depth located within the north eastern axis of the study area. The analytical signal amplitude map highlights the discontinuities or boundaries of the anomalous (granitic) body. It also enhances variations in the magnetic properties of the magnetic sources within the study area. The analytical signal amplitude map gave figures that range from 0.001 to about 0.047 nT/m. The map of the first vertical derivative depicts the near surface geological features such as fold, faults and geological structures within the trough. It is observed from the map of the first vertical derivative that most of the structures are trending in NE-SW (northeast to southwest), while some trends in NW-SE (northwest to southeast) directions. The major fault in the study area trends E-W (east to west) direction and these trends also conform to the trends indicated by the Rose diagram. The study also identified areas of high sedimentary thickness which could favour accumulation of hydrocarbon within the trough.

Key words: Analytical signal amplitude, first vertical derivative, Rose diagram, power spectrum.

INTRODUCTION

Africa, developed and other developing parts of the world in which Nigeria is included and other private economic investors have made use of aeromagnetic surveying technique in exploration for oil and gas and to geologically map strong magnetic basement at regional scale. They also employ aeromagnetic surveying in mapping magnetic

*Corresponding author. E-mail: ebukajohn421@gmail.com.

sedimentary contacts that are weak at a local scale. Aeromagnetic data has enabled researchers to depict the location and trends of intrasedimentary faults, folds, geological contacts, lineaments and other geological structures that can host the available mineral resources that are distributed across the globe. Nigeria as a country is blessed with so many mineral resources such as platinum, kaolin, coal, columbite, iron, limestone, tantalite, gypsum, diamond, and gold (Usman et al., 2018), if the available mineral resources are exploited, extracted and utilized, it will reduce the country's over dependency on crude oil and it will also contribute to the growth of national economy.

Airborne geophysical surveying which is assumed to be the oldest potential geophysical method involves the measuring of variations of various geochemical or physical anomalies of the earth including density, radioactive element concentration, electric powered conductivity and distribution of magnetic minerals. Various sedimentary basins normally have magnetic anomalies that usually arise from secondary mineralization alongside fault axis and it can be depicted on the aeromagnetic maps as surface linear characteristics.

Geophysical survey results are used to locate structures of geological interest and also to correlate spatial variations between rock properties and geology (Priscillia, Abu and Osagie, ing2021). Having a good knowledge of the origin and nature of mineralization is very vital in mineral exploration because mineral resources are structurally controlled and associated with geological structures such as faults, folds, fractures and shear zones. Delineating these structures helps in determining the trends of the available geological structures, the mineral and mining potentials of the region.

The aim of this present research is to delineate basement configuration and structural trends which controls mineralization in the Lower Benue Trough. This could be achieved by identifying the available lineaments, delineating the geological structures that host potential minerals, determining the depth of the structures and sedimentary thickness of the sub-basin.

Location and geology of the study area

Figure 1 shows the map of the location of the area under study. The area lies within Latitudes 6° 00^1N and 7° 20^1N and longitudes 10° 30^1 E and 11° 10^1E and covers an area of about 10, 952 km^2. The following towns lie within the study area: Obudu, Markurdi, Gboko, Ejekwe, Ogoja, Agana, Oturkpo, Akwana and Katsina-Ala.

Generally, the area under study is being underlain by the Asu River group which is known to be the first clastic fill of the Lower Benue Trough according to Petters and Ekweozor (1965). The Asu River group which are found in the Abakaliki-Afikpo basins is Albian to Cenomanian in age and they comprise fluvial regressive arkosic sandstones that are lie directly on the crystalline basement. The Asu River Group is being overlain by the Ezeaku Formation which is transgressive in nature and Turonian in age. It consists of siltstones and black shale that rests uncomformably at the Gneiss which is Precambrian in age and located at the north of Ugep (Arinze and Emedo, 2020).

METHODOLOGY

Nine sheets of Aeromagnetic data that is made up of sheet numbers 289 (Ejekwe), 291 (Obudu), 290 (Ogoja), 250 (Agana), 271 (Gboko), 251 (Makurdi), 272 (Katsina-Ala), 252 (Akwana), and 270 (Oturkpo) were gotten from the office of Geological Survey Agency of Nigeria. The survey was originally carried out in the year 2006-2007 by Fugro Airbone Survey. The survey was done on a scale of 1:250,000 with a line spacing of 500 m and flight elevation of 150 m above sea level along Northwest-Southeast lines. The data interpretations include the following steps:

(a) Digitization of Aeromagnetic data using potential field software like Oasis Montaj 8.3, USGS version 2.0.
(b) Residual separation using polynomial filtering.
(c) Production of map of the magnetic anomaly.
(d) Modelling and production of anomalous maps like first vertical derivative map and general analysis of the results.

Fourier Transform analysis interpretation which is applied in regularly spaced data (Abraham et al., 2022, 2023; Ikumbur et al., 2019, 2023; Onwuemesi, 1997) was performed for further analysis. Leu and Bhattacharyya (1975) method was applied on the spectral analysis results in order to calculate the centroid depth (Zo), depth to the top (Zt) and depth to the bottom of the magnetic sources (Zb).

Firstly, the (Zo) which is the centroid depth to the magnetic source is calcuated using the slope of the longest wavelength in the spectrum. It is expressed as:

$$In\left[\frac{\rho(\sqrt{S})}{/S/}\right] = InA - 2\pi/S/Z_o$$

where P - Represent the natural log of amplitude of the anomaly, /**s**/ - Represent the wave number, and A - Represent a constant.

Secondly, depth to the top of the anomaly (Zt) is derived from the second to the longest wavelength slope of spectral segment (Usman et al., 2023; Okonkwo et al., 2012; Okubo et al., 1985) and it is expressed as:

$$In\left[\frac{\rho(\sqrt{S})}{/S/}\right] = InB - 2\pi/S/Z_t$$

where B represents the sum of constants independent of /s/.

Finally, the depth to the bottom of the anomaly (Zb) according to(Usman et al., 2019 and Leu and Bhattacharyya (1975) is calculated as:

$$Z_b = 2Z_o - Z_t$$

Spectral analysis was equally used to establish a Power Spectrum from the total intensity field. The first vertical derivative which expresses the vertical gradients of the anomalous body was also performed from the spectral analysis. The analytical signal

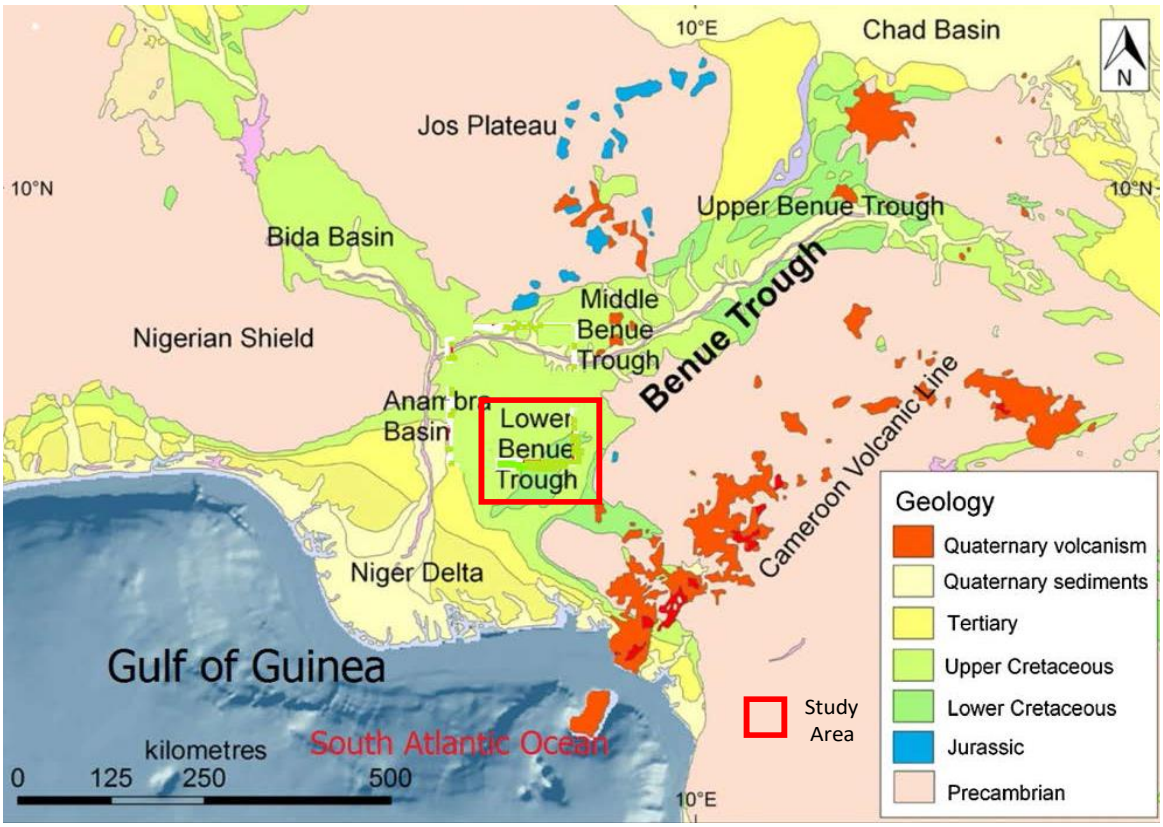

Figure 1. Geological Outcrop of the Benue Trough. (American Geoscience Institute (2014).

amplitude map was also produced from the spectral analysis according to Okonkwo et al. (2012) and Ikumbur et al. (2013).

RESULTS AND DISCUSSION

Qualitative interpretation

Shuttle Radar Topographic Mission map (Figure 2) explains the nature of the topography within study area. The elevation values within the study area ranges from about 345.1 to 661.0 m. The areas associated with low to moderate elevations are within the south western towards the north western parts of the map represented. While the highest elevations are associated within the eastern (north and south) parts of the study area.

The total magnetic intensity map (Figure 3) shows the rock types that is causing the anomaly within the basement, it also displays on a larger scale geological features such as geometry and configuration of the basin. The total magnetic intensity field value ranges from 31893 to 32205nT. The total magnetic intensity field map shows areas with low and high magnetic fields. Higher magnetic field intensity was indicated within the north eastern and north western parts of the displayed map. This was also accompanied by evidence of numerous bodies that is causing anomaly within those areas. The contour lines are spaced closely within those areas indicating a shallow depth to the basement rocks. The central and south western part of the map has relatively low magnetic field values and the contours within these areas are widely spaced indicating higher depth to the basement rocks.

Figure 4 shows the map of the residual magnetic field intensity of the study area. Values of the residual magnetic intensity field vary from -123.3 to 86.1 nT and the displayed map shows both low and high magnetic intensity field areas. The north eastern and north western areas of the map show evidence of higher magnetic fields. While the central and south western parts of the map show evidence of low magnetic field intensity values. It can also be observed from the map that the areas with higher magnetic intensity values has contours that are closely spaced indicating shallow depth to the basement and numerous anomalous bodies. While, the areas with low magnetic intensity values has widely spaced contours which signifies that the depth to the basement is relatively deeper. The study area has a major fault that is trending E-W (east-West) and other minor faults that equally trend in similar direction to the major fault according to Usman et al. (2023) and Nasir et al. (2022).

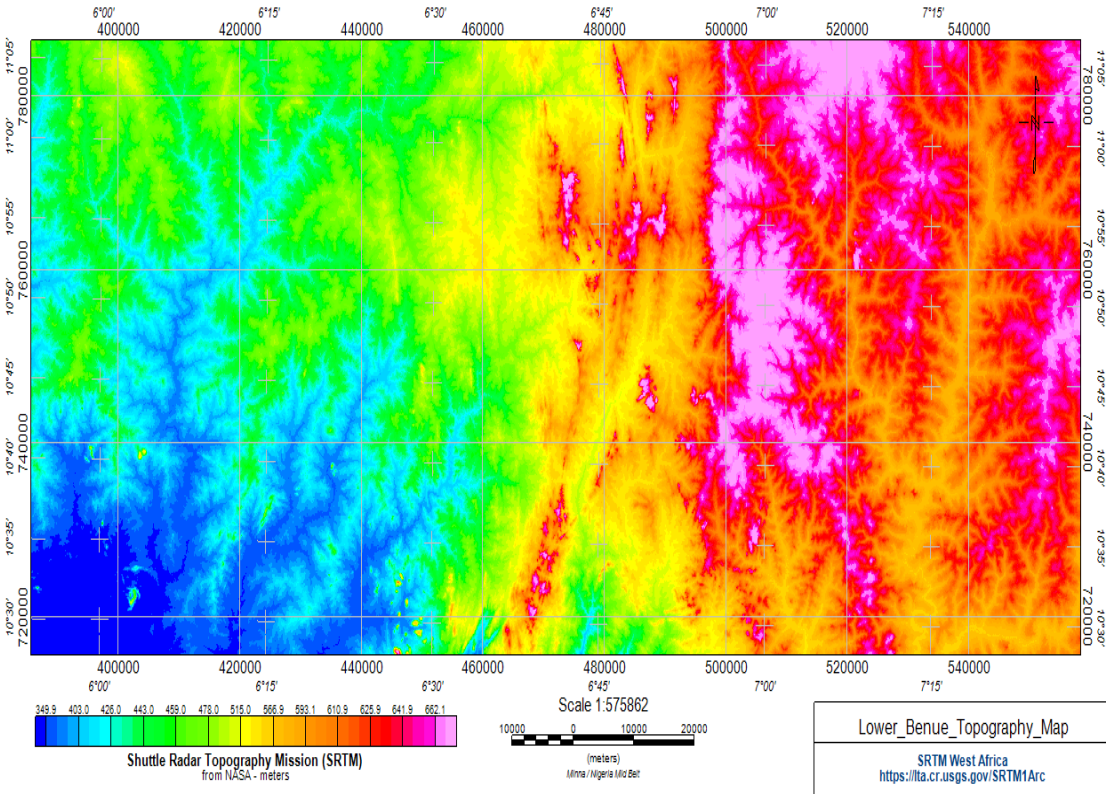

Figure 2. Map of the shuttle radar topographic mission of the study area.

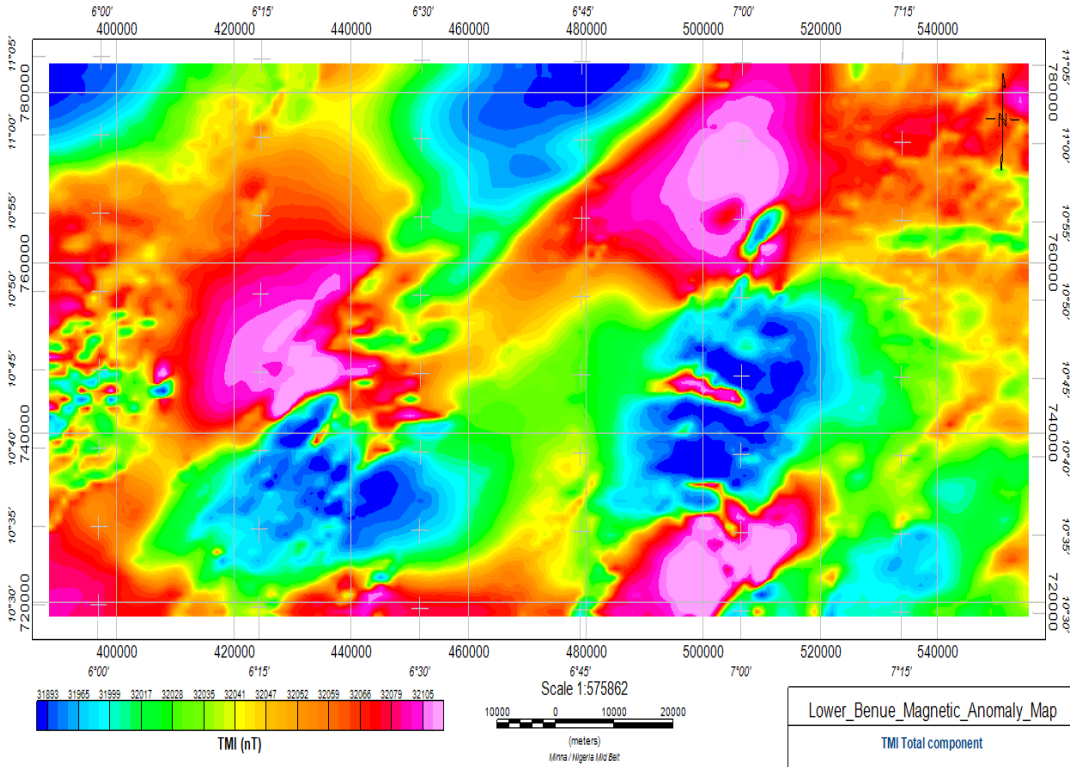

Figure 3. Map of the total magnetic intensity of the study area.

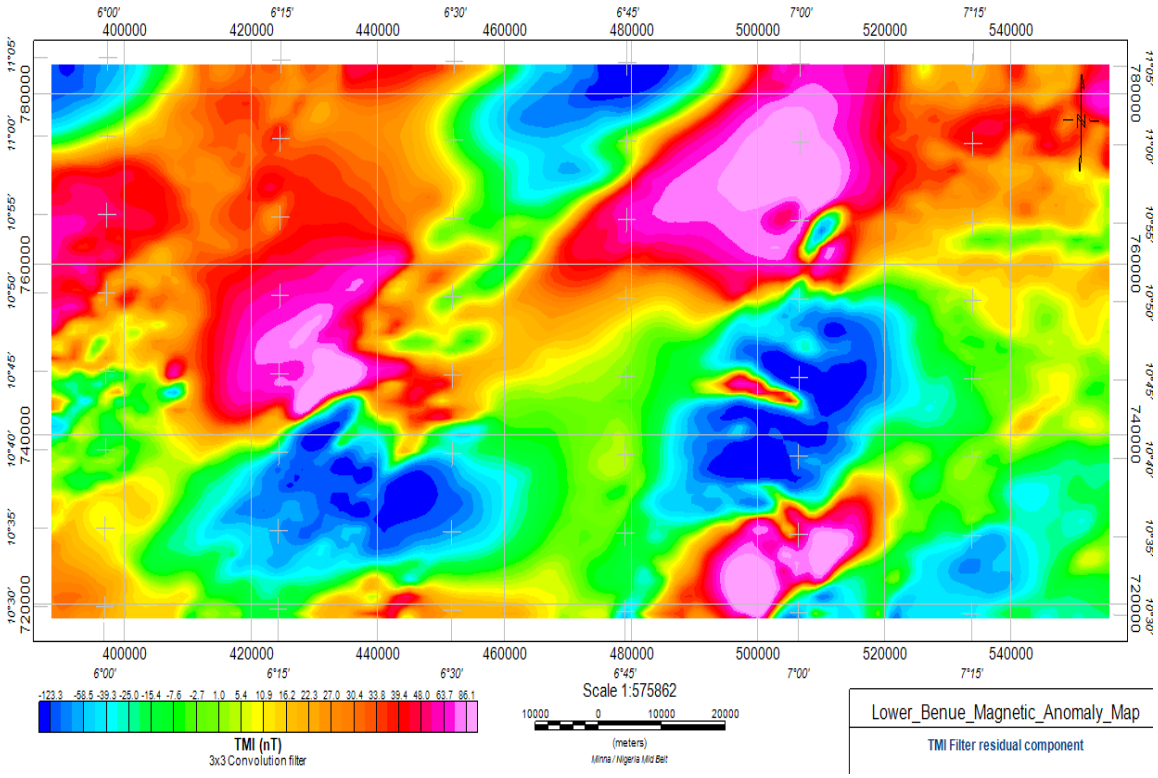

Figure 4. Map of the filtered residual magnetic intensity of the study area.

Figure 5 shows the map of the analytical signal amplitude within the study area. The analytical signal amplitude map depicts the exact boundary of granitic (magnetic) bodies. The values of the analytical signal amplitude ranges from 0.001 to 0.047 nT/m. According to Telford et al. (1990), rocks that are rich in ferromagnesian and minor felsic minerals, are usually associated with areas of high magnetic fields. The areas with high analytical signal amplitude from the map with a value of about 0.010 to 0.047 nT/m are related to ophiolotic serpentine, ophioliticmeta gabbro and gabbro rocks as these rocks contain ferromagnesian in large quantities and equally has large amount of felsic minerals. While the areas with low analytical signal amplitude with value range of about 0.001 to 0.006 amplitude (nT/m) are associated with granite, metasediments and clastic sediments as these rocks has quartz that is greater than 60% (Okonkwo et al., 2021; Telford et al., 1990).

Figure 6 shows the first vertical derivative map of the study area. The first vertical derivative map depicts surface features like faults, folds and other structures associated within the study area. The displayed map also gives the trend direction of the major fault which is East to West direction (east-west) according to Abraham et al. (2023) and Chinwuko et al. (2012, 2014). Other structures in the map trends NE-SW (northeast to southwest) while some trend NW-SE (northwest to southeast). These trends also conform to the trend indicated by the Rose diagram in Figure 8, for the altitude of the anticlinal structures.

From the Rose diagram represented in Figure 7, it can be observed that majority of the structures within the study area trends in NE-SW (northeast to southwest) while some trend NW-SE (northwest to southeast). Some also trend in west to eastern direction.

Quantitative interpretation of aeromagnetic data

From the residual map produced, 5 profile lines which are in perpendicular to the direction of the magnetic anomalies were taken. The lines were labelled A-A^1, B-B^1, C-C^1, D-D^1, and E-E^1 (Figure 8). The profile lines yielded 24 anomalies in total and spectral analysis were carried out on the produced anomalies in order to get the estimated depth to the top and bottom of the anomaly (Figure 9 and Tables 1 and 2).

Figure 10 represents the map showing thedepth to the top of the anomaly within the study area. It can be observed from the displayed map, that the deepest depth to the top of the anomalous body which is about 12 km is associated within the south western and north western parts of the study area. While, the north eastern part of the study area depicts shallow depth to the top of the anomalous body.

Figure 11 represents the map showing the depth to the

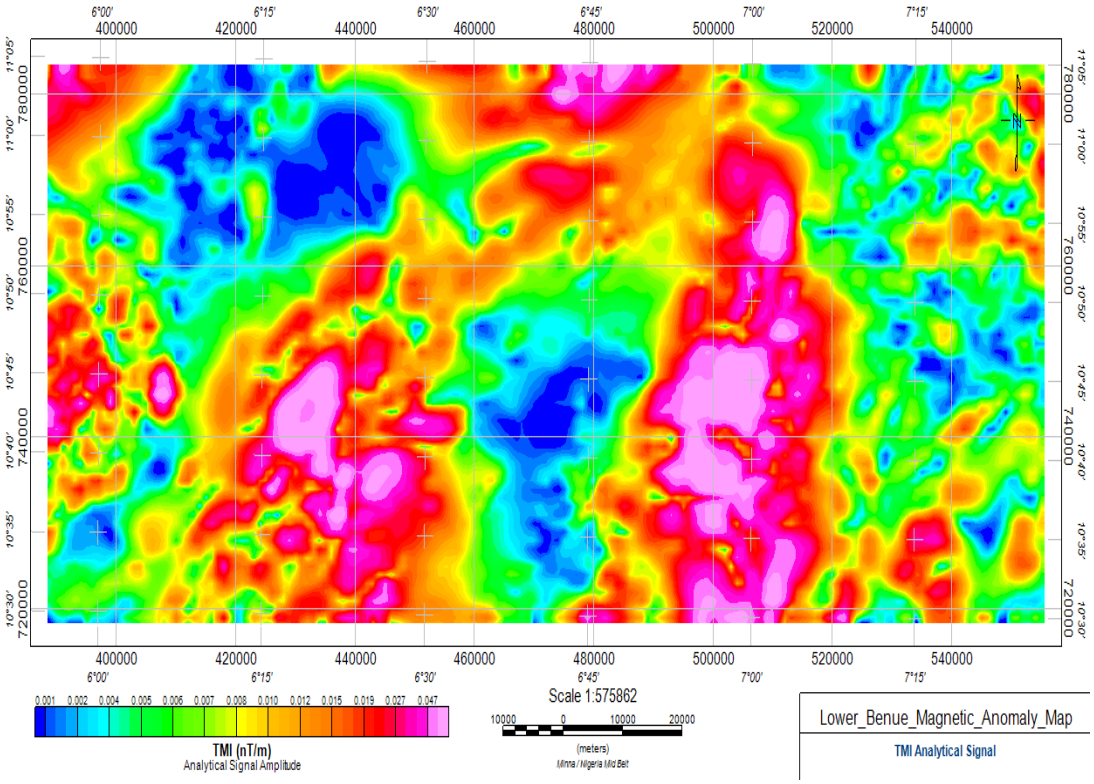

Figure 5. Map showing the analytical signal amplitude of the study area.

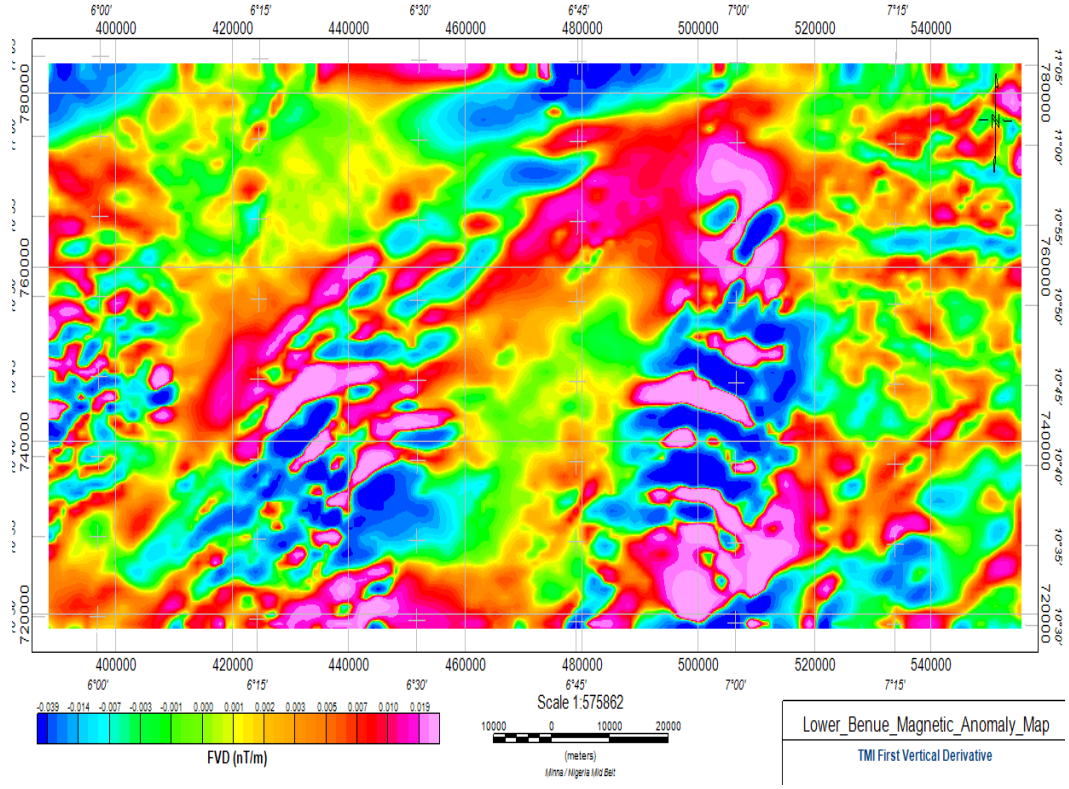

Figure 6. Map of the first vertical derivative of the study area.

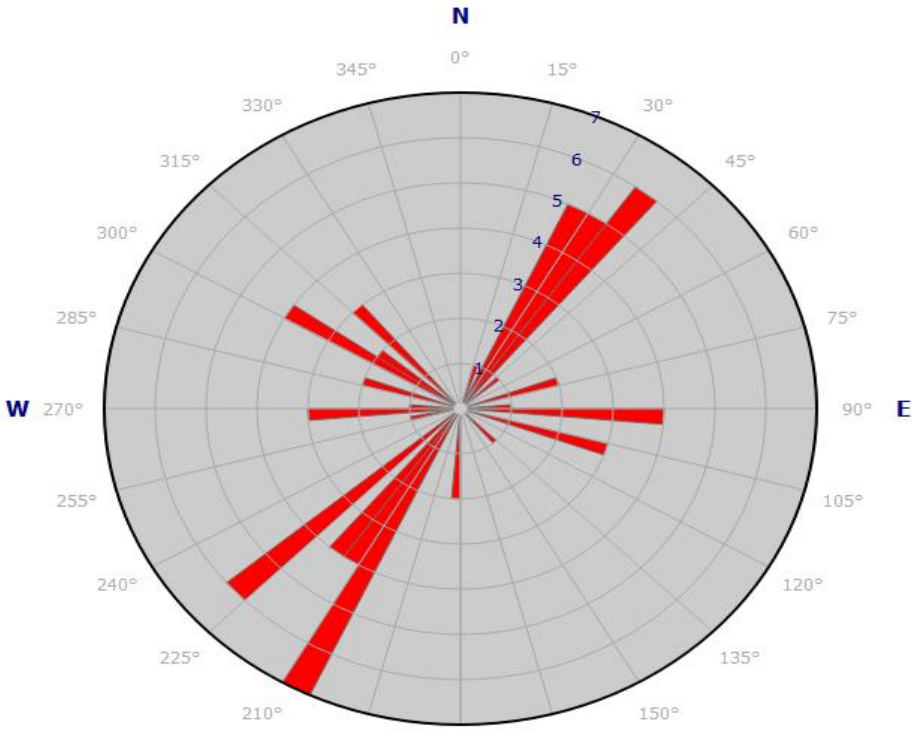

Figure 7. Rose diagram for the attitude of the anticlinical structures.

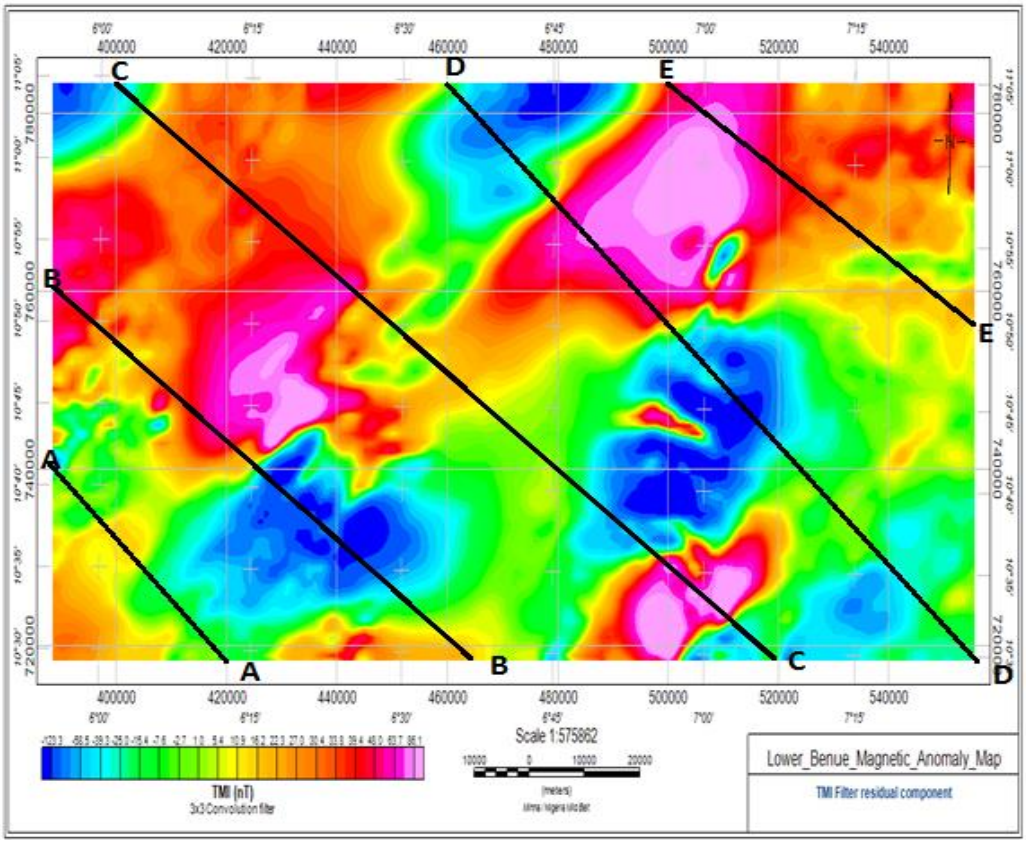

Figure 8. Residual map of the study area showing the profile lines.

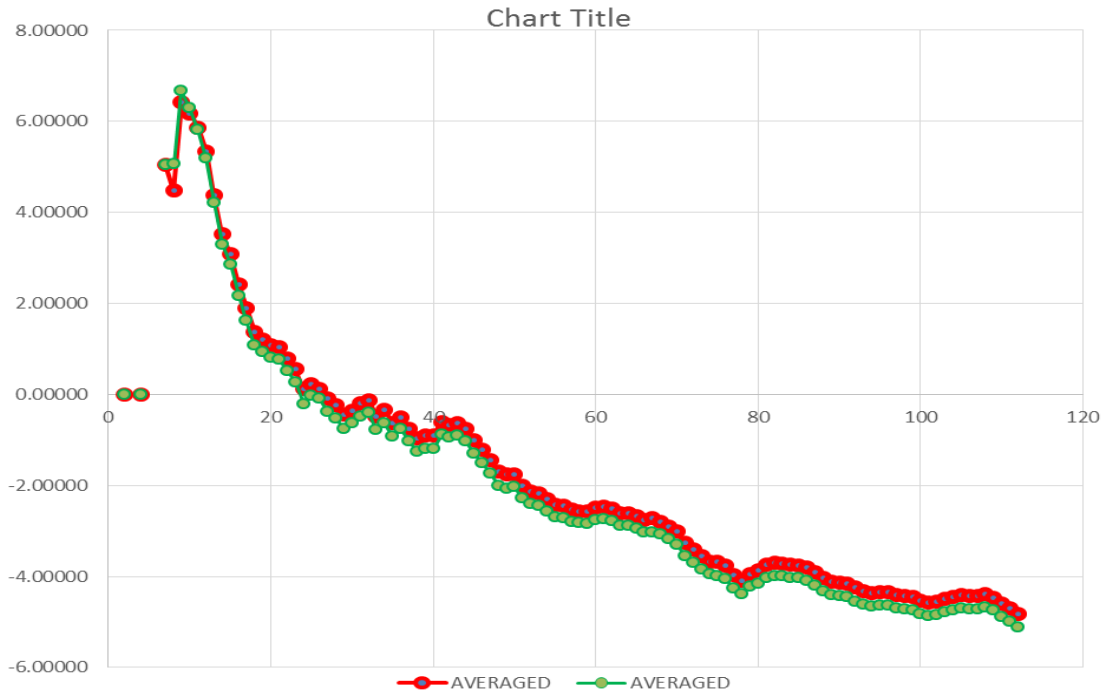

Figure 9. Power spectrum of the residual anomalous data.

Table 1. Results of the Analysis from the profile lines.

Profile A-A^{I}		Profile B-B^{I}		Profile C-C^{I}		Profile D-D^{I}		Profile E-E^{I}	
x(km)	y(km)	x(km)	y(km)	x(km)	y(km)	x(km)	y(km)	x(km)	y(km)
0	41	0	81	0	0	0	101	0	81
0.2	21	0.26	101	0.5	0.1	0.5	81	0.26	101
0.26	21	0.4	121	0.66	21	1.0	81	0.6	101
0.8	41	0.36	141	0.86	41	1.01	101	0.66	101
0.86	61	0.6	161	1.0	61	1.4	101	1.26	101
1.0	61	0.7	161	1.6	61	1.6	81	1.3	81
1.3	61	0.76	141	1.7	81	1.7	61	1.9	61
1.26	41	1.2	121	2.0	81	1.8	41	2.1	61
1.44	21	1.26	141	2.26	61	2.3	21	2.17	41
1.66	21	1.6	142	2.7	62	2.46	21	2.4	41
1.89	21	1.76	121	3.3	79	3.0	42	2.6	61
2	21	2.0	102	3.8	81	3.8	22	3.16	61
		2.76	81	3.7	99.9	4.2	21	4.0	41
		2.87	61	5.0	101	4.3	0	4.6	42
		3.1	41	6.76	101	4.7	-42	4.7	41
		3.7	42	7.3	81	5.1	-42	5.1	21
		4.77	81	8.1	81	5.27	0	5.45	0
		5.25	100	8.6	80	5.4	-20	5.6	-20
		5.26	101	8.9	81	5.6	-41	5.76	-41
		5.76	81	9.8	62	5.67	0	6.1	-62
		6	62	11	61	7	41	6.3	-61
		6.35	41	10.15	82	6.35	101	6.55	-42
		6.6	21	10.6	81	6.8	102	6.85	-22
		6.85	0	10.85	60	6.85	81	7.0	0
		7	-21	12	41	7.26	81	7.1	21

Table 1. Cont'd

7.2	-42	11.35	42	7.8	81	7.6	41
7.3	-41	11.7	21	8.3	101	7.7	62
7.4	-21	13	-21	8.6	102	8.45	82
7.7	0			9.0	82	8.8	102
7.85	22			9.45	61	9.35	102
7.75	41			11	42	9.45	81
8.2	61			10.3	42	9.6	61
				11.4	61	11	41
				12.9	61	12	42
				12.7	41	12.1	62
				12.8	22	12.2	81
				14	0	12.8	81
				13.2	-20	13.2	61
				13.3	-21	13.4	41
				13.6	-21	13.3	22
				13.85	-21	13.6	21
				14.3	0	13.9	41
				14.35	21	13.7	61
				14.8	41	13.7	81
				14.5	41	14	81
				14.85	21		
				15.0	-21		
				15.25	0		
				15.4	61		
				15.6	81		
				15.85	81		

Source: Chukwudi and Chukwuebuka (2023).

Table 2. Depth to the top and bottom of the anomaly from the spectral analysis.

Anomalies	Depth to the top (km)	Depth to the bottom (km)
1	12.77460	12.2
2	11.67320	13.13
3	9.93425	8.76
4	9.29714	10.53
5	2.61886	5.76
6	4.04175	5.14
7	4.16683	4.81
8	2.78819	5.76
9	1.76618	6.09
10	1.83936	9.06
11	2.89119	3.08
12	2.38351	2.79
13	0.67320	1.38
14	0.71833	9.88
15	1.81228	8.78
16	1.46625	6.14
17	1.19508	7.96
18	2.03137	8.12
19	2.00309	54.61
20	1.21583	9.02

Table 2. Cont'd

21	2.10640	8.34
22	2.72369	9.07
23	2.93912	9.56
24	2.64870	4.98
Average	3.65452	9.372917

Source: Chukwudi and Chukwuebuka (2023).

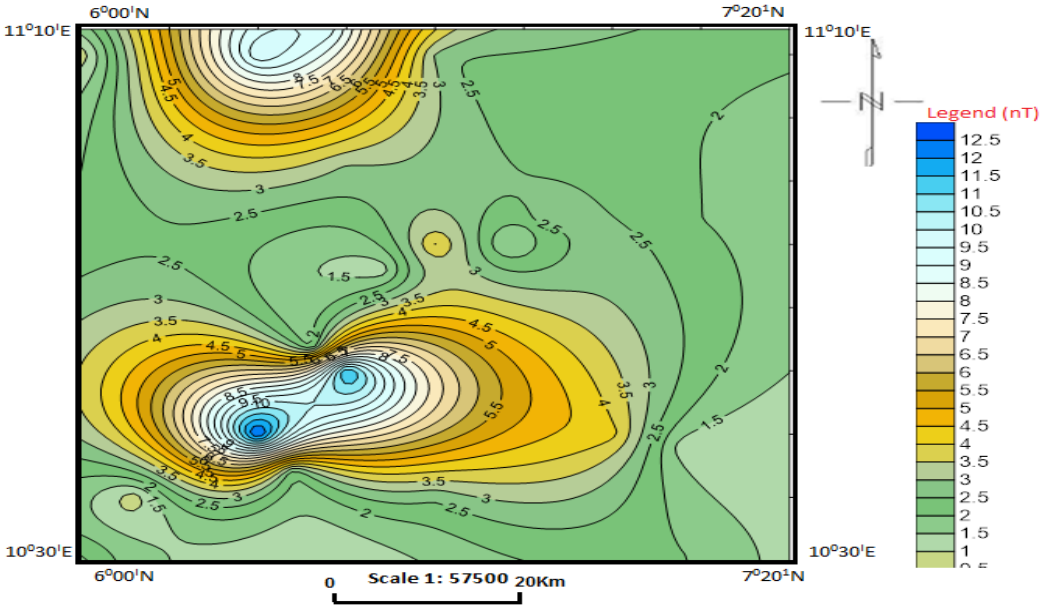

Figure 10. Depth to the top of the anomalous body map of the study area (Contour interval~ 1 km).

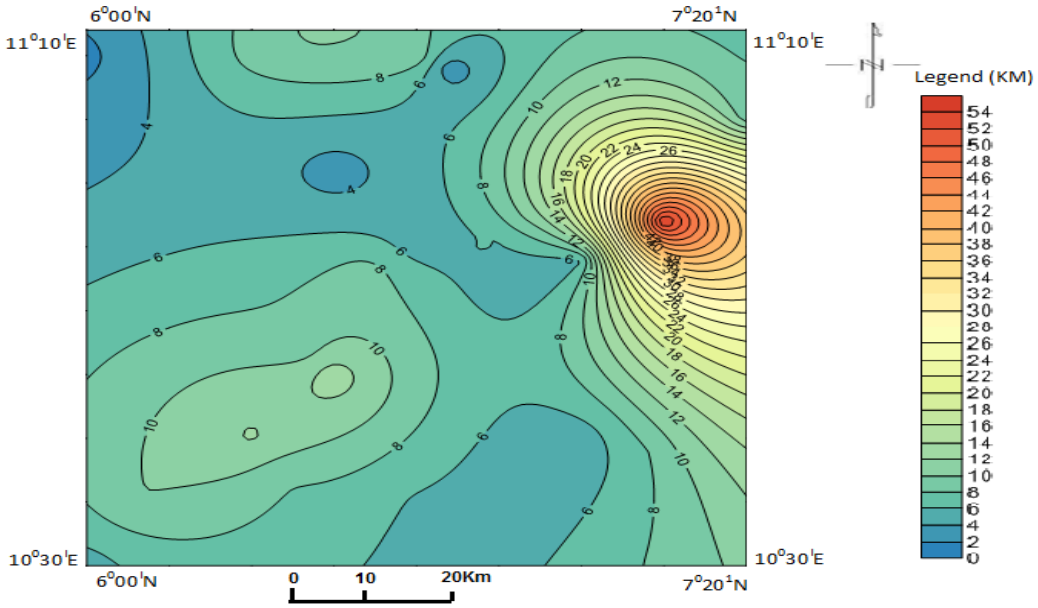

Scale: 1: 57500

Figure 11. Depth to the bottom of the anomalous body map of the study area (Contour interval~ 1 km).

bottom of the anomaly of the study area. From the map, the north-eastern parts are associated with the deepest depth to the bottom of the anomaly and the depth is estimated to be about 20 to 50 km. While the other parts of the map represent shallow to moderate depth to the bottom of the anomalous body.

Conclusion

Generally, the total magnetic anomaly and the residual magnetic anomaly have values that range from 31893 to 32205 and -123.3 to 86.1 nT, respectively. Both maps depict that the north eastern and north western parts of the study area are associated with higher magnetic intensities and the anomalous bodies within these areas are numerous. The maps also indicate that the contours in these areas are close to each other indicating shallow depth to the basement rocks. Five profile lines which were in perpendicular to the direction of the magnetic anomalies were drawn on the residual filtered map in order to estimate the depths to the top and bottom of the anomalous bodies using the Discrete Fourier Transform of Aeromagnetic data. Both maps to the top and bottom of the anomaly indicated high sedimentary thicknesses. From the first vertical derivative map and the map showing the analytical signal amplitude, it is observed that the geological structures present in the study area are mainly dykes, sills, intrusive structures, fault, joints and mineralization veins which trend mostly in NE-SW (northeast to southwest) direction while some trend in NW-SE (northwest to southeast) direction. The major fault in the study area trends in E-W (east to west) direction according to Usman et al. (2018). The study area is associated with high sedimentary thickness. There is also presence of geological structures which could encourage the accumulation of hydrocarbon making possible the availability of solid minerals within the study area.

CONFLICT OF INTERESTS

The authors have not declared any conflict of interests.

REFERENCES

Abraham EM, Mkpuma RO, Usman AO, Gwazah CA, Mgbeafuruike EU (2022) Mapping of mineral deposits within granitic rocks by aeromagnetic data-a case study from Northern Nigeria. Arabian Journal of Geosciences 15:1656

Abraham EM, Usman AO, Chıma KI, Azuoko GB, Ikeazota II (2023) Magnetic inversion modelling of subsurface geologic structures for mineral deposits mapping in southeastern Nigeria. Bulletin of the Mineral Research and Exploration 1-1. DOI: 10.19111/bulletinofmre.1267876

Arinze I, Emedo C (2020). Integrated geophysical Investigation for shallow – Scale massive (Pb-Zn) sulphide and barite Exploration in Abakaliki and Obubra mining Districts (AOMD), Southeastern Nigeria. Mining, Metallurgy and Exploration 38(1):381-395.

Chinwuko AI, Onwuemesi AG, Anakwuba EK, Nwokeabia NC (2012). Interpretation of Aeromagnetic anomalies over parts of Upper Benue Trough and Southern Chad Basin, Nigeria. Advances in Applied Science Research 3(3):1757-1766.

Chinwuko AI, Usman AO, Onwuemesi AG, Anakwuba EK, Okonkwo CC, Ikumbur EB (2014). Interpretations of aeromagnetic data over lokoja and environs, Nigeria. International Journal of Advanced Geosciences 2 (2):66- 71.

Chukwudi CC. Chukwuebuka JM (2023). Evaluation of Geothermal energy potentials in parts of the Lower Benue Trough, Nigeria, using Aeromagnetic data. Journal of Earth Sciences and Geotechnical Engineering 13 (2):1-22.

Ikumbur EB, Chinwuko AI, Ogah VE, Akiishi M, Usman AO, Udoh AC (2019). Curie-Temperature Depth and Heat Flow Deduced from Spectral Analysis of Aeromagnetic Data over the Southern Bida Basin, West-Central Nigeria. Geosciences 9(2):50-56.

Ikumbur EB, Onwuemesi AG, Anakwuba EK, Chinwuko AI, Usman AO, and Okonkwo CC (2013). Spectral Analysis of Aeromagnetic Data over Part of the Southern Bida Basin, West-Central Nigeria International Journal of Fundamental Physical Sciences 3(2):27-31.

Ikumbur EB, Onwuemesi AG, Anakwuba EK, Chinwuko AI, Usman AO (2023). Evaluation of Geothermal Energy Potential of Parts of the Middle Benue Trough Nigeria: Aeromagnetic and Aeroradiometric Approach. Iranian Journal of Geophysics 16(4):7-52.

Leu LK, Bhattacharyya BK (1975). Spectral analysis of gravity and magnetic anomalies due two-dimensional structures. Geophysics 40:993-1031.

Nasir NA, Ene KO, Oluwatoyin O (2022). Evaluation of structural framework and depth estimates using High resolution Airborne magnetic data over some parts of Middle Benue Trough, Nigeria. International Journal of Geosciences 13:557-575.

Okonkwo CC, Onwuemesi AG, Anakwuba EK, Chinwuko AI, Ikumbur BE, Usman AO (2012) Aeromagnetic Interpretation over Maiduguri and Environs of Southern Chad Basin, Nigeria. Journal of Earth Sciences and Geotechnical Engineering 2(3):77-93.

Okonkwo CC, Onwuemesi AG, Anakwuba EK, Chinwuko AI, Okeke SO, Usman AO (2021) Evaluation of Thermomagnetic Properties and Geothermal Energy Potential in Parts of Bida Basin, Nigeria, Using Spectral analysis. Bulletin of the Mineral Research and Exploration 165:13-30.

Onwuemesi AG (1997). One dimensional spectral analysis of aeromagnetic anomalies and curie depth isotherm in the Anambra Basin of Nigeria. Journal of Geodynamics 23(2):95-107.

Petters SW, Ekweozor CM (1965). Petroleum Geology of the Benue Trough and Southeastern Chad Basin, Nigeria. American Association of Petroleum Geologists Bulletin 66:1141-1149.

Telford WM, Geldart IP, Sheriff RE (1990). Applied Geophysics, Second Edition, Springer, Berlin 770 p.

Usman AO, Chinwuko AI, Azuoko GB, Ekwe AC, Abraham EM, Chizoba CJ (2023). Geo-morphological mapping of the Basin configuration of parts of Southern Nupe Basin, Nigeria using High-Resolution Aeromagnetic and core drill dataset. Iranian Journal of Geophysics, Accepted April 8th 2023

Usman AO, Ezeh CC, Chinwuko AI (2019). Estimation of Geothermal gradient and Curie Point Depth for Delineating Hydrocarbon potentials zones over Southern Bida Basin, Northwestern Nigeria. Development Journal of Science and Technology Research (DJOSTRR) 8(1):105-119

Usman, AO, Ezeh CC, Chinwuko AI (2018). Integration of Aeromagnetic Interpretation and Induced Polarization methods in delineating mineral deposits and Basement configuration within SouthernBida Basin, North- West Nigeria. Journal of Geology and Geophysics 7(449):2381-8719.